

EVALUATION OF CORROSION RESISTANCE OF TITANIUM ALLOYS USED FOR MEDICAL IMPLANTS

The study presents the results of investigations of modeling the usable properties of implant surfaces made of Ti6Al7Nb alloy, using the example of a dynamic hip screw (DHS) applied in surgical treatment of intertrochanteric femoral neck fractures. Numerical simulation has been performed for the model load of femoral fixation with DHS screw. The load simulation results provided the basis to select mechanical properties of the fixator elements and to define those fixation areas which are mostly susceptible to development of corrosion. The surfaces of Ti6Al7Nb alloy were ground, vibro-abrasive machined, mechanically polished, sandblasted, anode oxidized at different voltage values and steam sterilized. Results of surface topography evaluation, resistance to pitting and crevice corrosion as well as degradation kinetics of the outer layer were presented. Usability of the formed passive layer in clinical applications was evaluated through wear and corrosion tests of the femoral fixation model. The test results proved usefulness of the proposed surface modification methods for clinical application of different size and shape implants

Keywords: metallic biomaterials, titanium alloys, corrosion resistance, mechanical processing, anodic oxidation

1. Introduction

Treatment of fractures and bone reconstruction employs structurally complex implants made of metal biomaterials. The surgical techniques and biomechanical improvements in the area of the trauma contributes to differentiation of corrosion processes in individual areas of the implants. Recognition of the corrosion processes provides basis for modification of their surface layers.

Selection of a metal biomaterial for an implant for a given functional use is determined by: the structural profile of an implant, the surgical technique, duration of use as well as biomechanical properties of the reconstructed tissues. Interrelations among those factors are complex and make it difficult to choose proper mechanical and physicochemical properties of a metal biomaterial. Such properties also need to comply with the surgical technique, often involving pre-operative modeling of the implants [1, 2].

The shape and size of bone fixator elements may be optimized through numerical simulation [3,4]. The determined mechanical characteristics of the loaded models of bone fixation provide a basic criterion for selection of a metal biomaterial and its mechanical properties. Bone fixation is supposed to stabilize the fracture and to ensure conditions for physiological stimulation of anastomosis. The range of stress and displacement within the fixation are must not exceed the limit values, relating to both, the tissues and the metal material. Ensuring the demanded deformation capacity of the loaded stabilization system must correlate with mechanical properties of the protective passive layers formed on the implant surface. Breaking continuity of such layers may result in initiation of corrosion processes [2].

If a society is getting older, the most prevalent traumas

are fractures within the area of the proximal femur. Among the methods of fixation of such intertrochanteric fractures is the use a dynamic hip screw system (DHS). Made of austenitic steel, used mostly in short-term implants. This study proposes an alternative material, which is Ti6Al7Nb alloy. The alloy is a biomaterial designed for long-term implants. More and more clinical observations tend to report allergic response to titanium of its corrosion products. This calls for appropriate barrier layers on titanium alloy implants.

There are many methods available to modify the implant surface [5-8], however the most frequent procedure used to modify titanium alloy implant surfaces has been anode oxidation. Depending on the process parameters, the formed outer layers may show different chemical composition, thickness and morphology [9,10]. The basic factors to determine properties of the passive layer are the chemical composition of the bath and voltage of anode oxidizing. Another important factor is the type of processing preceding anode oxidation.

The study has proposed a universal technology for modification of the surface layer of on the Ti6Al7Nb alloy base. Such technology makes it possible to form a passive layer on implants of variable shape and size. Its usefulness has been proved during wear and corrosion tests of the fixation model of intertrochanteric femoral fractures, stabilized with DHS system.

2. Materials and methods

2.1. Numerical simulation

Numerical simulation of loading of the femoral fixation model, with the use of dynamic hip screw DHS (Fig. 1), was

* SILESIA UNIVERSITY OF TECHNOLOGY, DEPARTMENT OF ENGINEERING MATERIALS AND BIOMATERIALS, 40 ROOSEVELTA STR., 41-800 ZABRZE, POLAND

[#] Corresponding author: Janusz.Szewczenko@polsl.pl

performed in Ansys Workbench 13 environment. Evaluation comprised fixation of an intertrochanteric femoral neck fracture (Fig. 2). Preliminary tests included evaluation of a non-fractured femur.

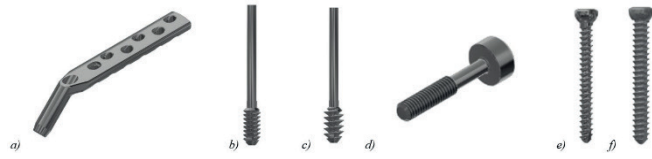


Fig. 1. Elements of Dynamic Hip Stabilizer which underwent numerical analysis: a) DHS plate, b) DHS bolt, thread diameter: 12.5 mm, c) DHS bolt, thread diameter: 16 mm, d) compression bolt, e) bone screws, diameter: 4.5 mm, f) bone screws, diameter: 5.5 mm

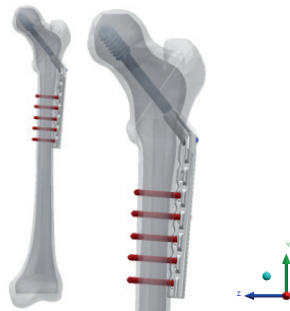


Fig. 2. Geometrical model of the system femur - dynamic hip screw, DHS

Fixation was performed with the use of DHS plate, with the neck section length, $L_s = 38$ mm, the plate length, $L = 105$ mm and the angle of 135° , developed by BHH Mikromed. DHS screws of thread diameter, $G = 12.5$ mm (standard DHS screw used in a normal, spongy bone) were used along with five bone screws of $BS = 4.5$ mm diameter. The width of the fracture fissure was $d = 0.2$ mm. For numerical calculations, mechanical properties specified in (Table 1) were assumed.

The following were assumed for the needs of the analysis:

- distal part of femur was immobilized by depriving the nodes situated along the plane of all the freedom degrees,
- the bone was loaded following Będziński model [14]. The values of forces assumed for the test corresponded to peak values reached when carrying a load with one limb by a walking person of 70 kg bodyweight.

2.2. Material testing

Used during the tests was Ti6Al7Nb alloy with chemical composition, structure and mechanical properties complying with ISO 5832-11 recommendations. The sample were mechanically pre-processed, including: grinding, vibro-abrasive machining, mechanical polishing and sandblasting. The finishing processes were anode oxidation and steam sterilization. Grinding made use of abrasive paper, subsequently of 120,130 and 600 grade. For vibro-abrasive machining, ceramic profiles and the wetting agent were used. Mechanical polishing made use of sisal brushes, linen disks and polishing paste. For sandblasting glass balls of diameter from 0.7 to 110 μm were used. Anodization was carried out with the use of electrolyte based on phosphorous and sulphuric acid at the voltage 57 V, 77 V, 87 V and 97 V. Steam sterilization was done at the temperature of 134°C and pressure of 2.1 bar, during 12 minutes.

Surface topography and roughness were evaluated with the use of atomic force microscope (AFM) NTegra Spectra by NT-MDT. For semi-contact topography, VIT_P silicone pins of resonance frequency 400 kHz were used.

Resistance to pitting and crevice corrosion were evaluated as per PN-EN ISO 10993-15 and ASTM F 746. Assays were carried out in Ringer solution of chemical composition: $\text{NaCl} - 8.6 \text{ g/dm}^3$, $\text{KCl} - 0.3 \text{ g/dm}^3$, $\text{CaCl}_2 \cdot 2\text{H}_2\text{O} - 0.33 \text{ g/dm}^3$, at the temperature $T = 37 \pm 1^\circ\text{C}$ and $\text{pH} = 6.9 \pm 0.2$. PGP201 potentiostat by Radiometer was used. The reference electrode was a saturates calomel electrode (SCE), and the supporting one, a platinum rod. Evaluation of pitting resistance was performed for sterilized samples (S) stored in 0.2 dm^3 Ringer solution, at the temperature $37 \pm 1^\circ\text{C}$ for 28 days. The rate of potential changes was 3 mV/s. During the tests of crevice corrosion resistance, the sterilized samples (S) were polarized with +800 mV potential, recording the current density curve in time function for 15 minutes.

Concentration of ions, which infiltrated Ringer solution from titanium alloys during 28 days, was determined by inductively coupled plasma – atomic emission spectrometry (ICP–AES).

In order to define usefulness of the formed layers for Ti6Al7Nb alloy implants, wear tests of femoral fixation with DHS screw were performed. The implants used were ground, vibro machined, mechanically polished, anode oxidised at 97V and steam sterilized.

TABLE 1

Mechanical properties assumed in the numerical analysis of the femur - DHS system

Element of a computing system			Mechanical properties				
E, [MPa]			E, [MPa]	ν	R_c , [MPa]	$R_{p0.2}$, [MPa]	R_m , [MPa]
ν							
Femur	Steam	[11]	17900	0.3	180	-	-
	Head	[12, 13]	17000	0.3	-	-	-
	Trabecular bone		900	0.3	-	-	-
	Early Stage of Fracture Healing		3	0.4	-	-	-
Ti6Al7Nb alloy		ISO 5832-11	110000	0.33	-	780	860
E - Young's modulus, ν - Poisson's ratio, R_c - Ultimate compressive strength, $R_{p0.2}$ - Yield strenght, R_m - Ultimate tensile strength							

The femoral fixation model (by Sawbone) was made to comply with the demanded surgical technique. The model investigated corresponded to one applied for numerical simulation DH16 BS4.5x5. The models of femoral fixation were subjected to wear tests at low cycle number. The axial loads were within the range -50 N÷-1000 N. Following the wear tests the fixation models were placed in Ringer solution at temperature $T = 37 \pm 1^\circ\text{C}$ and $\text{pH} = 6.9 \pm 0.2$ for the period of 20 weeks. After exposure in corrosion environment the fixator elements were observed in a stereoscope microscope, SteREO Discovery V8 by Zeiss. Particular attention has been paid to areas of peak stress in the system elements determined by numerical simulation.

3. Results and discussion

3.1. Numerical simulation

Results of evaluation of displacement and reduced stress of the loaded femoral fixation are presented in Table 2 and in Fig. 3.

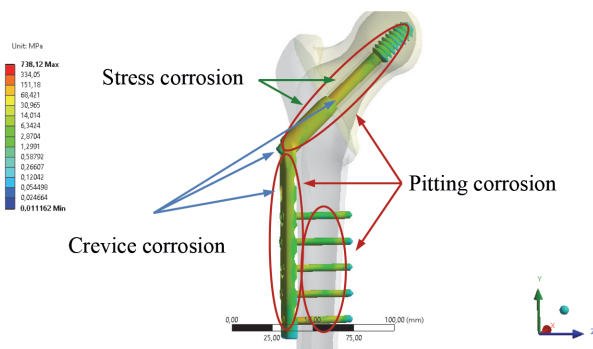


Fig. 3. Stress distribution in DHS fixator with the marked areas promoting initiation and development of different types of corrosion

In the model of a non-fractured femur, where no implant was applied, the proximal femur displaced by $L = 6.5 \text{ mm}$ which produced the stress $\sigma = 34 \text{ MPa}$.

Displacement values of the system femur - DHS screw were close to those obtained for a non-fractured bone and equaled $L = 7.42 \text{ mm}$. The evaluation results show that in the assessed model the peak stress in the fixator elements does not exceed the limit of plasticity of a metal material. Also no exceeded strength values were observed in the cortical bone and the spongy bone.

Peak stress values observed in the fixator elements were at the contact area of DHS screw and the DHS plate neck as well as in the screw sockets of the DHS plate. Moreover, stress accumulation was observed at the groove area where the core passes into the head. The obtained stress distribution in models of intertrochanteric femoral fracture fixation with DHS screw made of Ti6Al7Nb alloy are similar to the fixation models made of austenitic steel [12,13,15,16].

The peak stress areas are where a failure may occur due to mechanical load of the passive layer, likely to initiate corrosion. Such areas are at risk of development of crevice corrosion, pitting and wear corrosion.

3.2. Material testing

During observation of the surface of samples made of Ti6Al7Nb alloy, after grinding, vibro-machining polishing, sandblasting and anode oxidation at difference voltage and with the use of atomic force microscope, the parameter of roughness, S_a , was determined (Fig. 4). The values of the parameter depended on anode oxidation voltage and reached 216 nm, 249 nm, 257 nm and 270 nm, respectively for the voltage 57 V, 77 V, 87 V and 97 V. Along with the growth of anode oxidation voltage we observe increased roughness of the sample surface. Similar relation was observed in samples after different pre-conditioning (preceding anode oxidation and steam sterilization) procedures modifying the outer layer of titanium alloys [18].

Polarization curves of the oxidised and sterilized samples (S) as well as those after exposure to Ringer solution (28D), showed no hysteresis loop, regardless of the voltage applied. This proves effective passivation of the sample surface, throughout the measurement range. Polarization curves, obtained by Stern method within the range $\pm 10 \text{ mV}$, were used to determine the corrosion potential E_{corr} as well as polarization resistance R_p (Table 3). It was observed along with the growing anode oxidation voltage, the value of the corrosion potential of the samples after sterilization (S) increased while it was reduced for samples stored in Ringer solution (28D). Regardless of anode oxidation voltage, the growth of corrosion potential and polarization impedance, as resistance to sterilizes samples, was observed in all sampled stored in Ringer solution (28D). Similar relations were observed in samples after other pre-conditioning procedures, modifying the outer layer of titanium alloys [19,20].

TABLE 2

The results of the numerical analysis for the models

	Results for whole model			von Misses stress for individual parts of models σ , [MPa]						
	L [mm]	ϵ	σ [MPa]	σ_{fs}	σ_{fh}	σ_{fht}	σ_{DHS}	σ_{cs}	σ_{DHSp}	σ
Femur	6.50	0.00	34.20	-	-	-	-	-	-	-
Femur-DHS system	7.42	0.64	738	127	10	3	538	93	220	738

L – displacement, ϵ – von Misses strain, σ – von Misses stress, σ_{fs} – femur steam, σ_{fh} – femur head, σ_{fht} – femur head - trabecular bone, σ_{DHS} – DHS screw, σ_{cs} – compression screw, σ_{DHSp} – DHS plate, σ_{bs} – bone screws

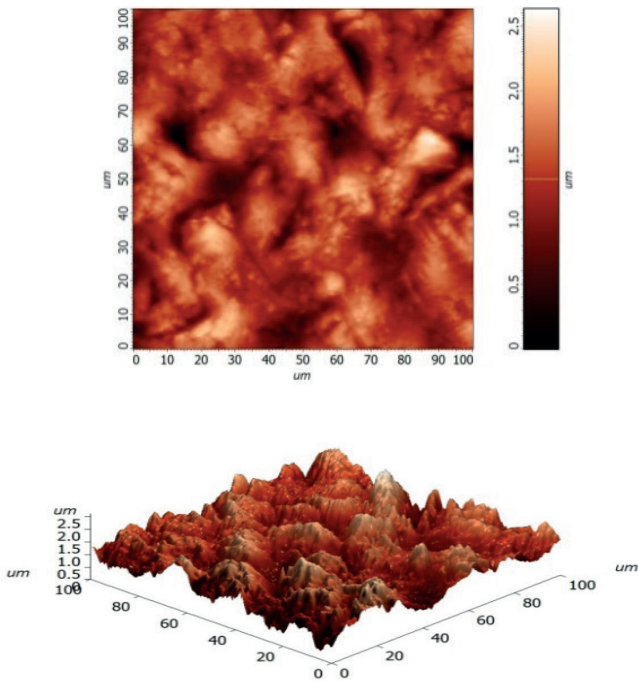


Fig. 4. Topography of the sample surface after anode oxidation at 97 V voltage (AFM)

All the sterilized samples, regardless of anode oxidation voltage were resistant to crevice corrosion.

Analysis of chemical composition of Ringer solution, in which Ti6Al7Nb alloy samples were kept, revealed the presence of Ti, Al and Nb ions. Concentration of ions which infiltrated the solution, was calculated as the mass of an element infiltrating from the unit of the sample surface (Table 4).

TABLE. 3

Corrosion potential and polarization resistance of Ti6Al7Nb alloy samples

Voltage	E_{corr} [mV]		R_p [$M\Omega\text{ cm}^2$]	
	S	28D	S	28D
57V	-242(42)	181(32)	0.68(11)	13.37(97)
77V	-204(49)	177(68)	0.62(24)	13.66(89)
87V	-194(39)	-18(21)	0.42(17)	4.76(76)
97V	-122(34)	-6(99)	1.34(36)	4.64(69)

TABLE 4

Density of metal ion mass infiltrating the solution.

Voltage	Ti [$\mu\text{g}/\text{cm}^2$]	Al [$\mu\text{g}/\text{cm}^2$]	Nb [$\mu\text{g}/\text{cm}^2$]
57V	10.390(16)	1.847(57)	1.961(98)
77V	9.183(68)	1.608(98)	1.946(88)
87V	7.222(99)	1.259(88)	1.753(36)
97V	4.584(88)	1.056(47)	1.608(26)

The solution was infiltrated mostly by the ions of titanium, with the lowest scores for niobium. Density of ion mass infiltrating the solution, depended on anode oxidation voltage. The lowest value was observed for 97V, while the highest for 57V.

Relation between the quantity of corrosion products infiltrating the solution from titanium alloy surface and

the voltage of anode oxidation is due to diverse thickness of the formed passive layer [18]. However, the most important factor is the method of pre-conditioning prior to anode oxidation [19].

Evaluation of degradation test of Ti6Al7Nb alloy samples with modified outer layer was the basis to select a modification variant for surfaces of elements of DHS fixation system. Selected were: grinding, vibro-machining, mechanical polishing, sandblasting, anode oxidation at 97 V and steam sterilization.

Few scratches were revealed on the surface of DHS fixator elements at the input stage (Fig. 5). After cyclic loading and storage in Ringer solution some mechanical failures were also notice (Fig. 6a). Failures due to cyclic load was observed in the areas of peak load, determined by numerical simulation (Figs. 4 and 6). Mechanical damage of the outer layer neither initiated nor contributed to the development of corrosion. This proves the ability of the outer passive layer to repassivate in the environment of physiological solutions.

4. Conclusions

The investigations carried out showed usefulness of the applied method of shaping the outer layer on the base of implants of Ti6Al7Nb with complex shape and size. The passive layer formed through grinding, vibro-machining, mechanical polishing, sandblasting and anode oxidation at 97V as well as steam sterilization, successfully protects the implants against pitting, crevice corrosion and the wear one, restricting the quantity of corrosion products infiltrating the external environment. Moreover, the passive layer is repassivated, is damaged.

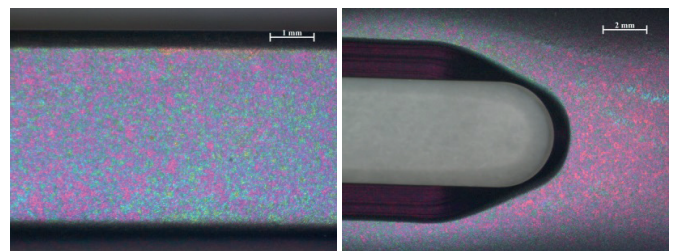
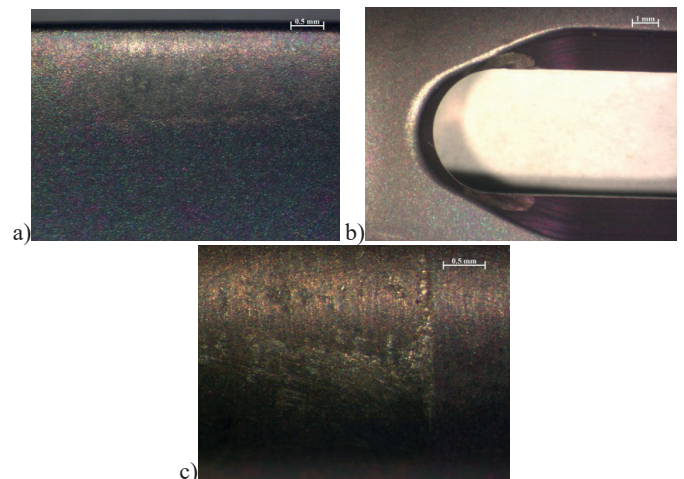


Fig. 5. The surface of DHS plate, anode oxidised at 97 V



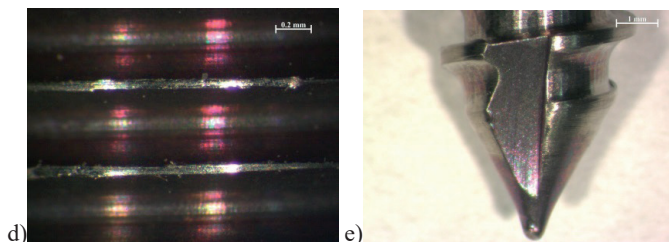


Fig. 6. Surface damage of DHS fixator element after wear tests and exposure to corrosion environment: a) DHS plate – abrasive damage in the bone-contacting area, b) DHS plate – plastic deformation in the bone screw socket area, c) DHS screw – abrasive damage in the area of contact with DHS plate, d) compression bolt – mechanical damage of the thread, e) bone screw- damage of the outer layer

REFERENCES

- [1] W. Kajzer, A. Kajzer, B. Gzik-Zroska, W. Wolański, I. Janicka, J. Dzieliński, Comparison of Numerical and Experimental Analysis of Plates Used in Treatment of Anterior Surface Deformity of Chest, in: E. Piętka, J. Kawa (Ed.): LNCS 7339, Springer-Verlag Berlin Heidelberg (2012)
- [2] A. Kajzer, W. Kajzer, B. Gzik-Zroska, W. Wolański, I. Janicka, J. Dzieliński, *Acta Bioeng Biomech.* **15**, 31, 13-121(2013).
- [3] M. Kiel, J. Marciniak, M. Basiaga, J. Szewczenko, Numerical Analysis of Spine Stabilizers on Lumbar Part of Spine. in: E. Piętka, J. Kawa (Ed.): *Advances in Intelligent Systems and Computing*, 69, Springer-Verlag Berlin Heidelberg (2010)
- [4] W. Walke, J. Marciniak, Z. Paszenda, M. Kaczmarek, J. Cieplak: Biomechanical behaviour of double threaded screw in tibia fixation. in: E. Piętka, J. Kawa (Ed.): *Advances in Soft Computing*, 47, Springer-Verlag Berlin Heidelberg, Berlin (2008).
- [5] E. Czarnowska, J. Morgiel, M. Ossowski, R. Major, T. Wierzchoń, *J. Nanosci. Nanotechnol.* **11**, 10, 8917-8923 (2011).
- [6] M. Basiaga, M. Staszuk, W. Walke, Z. Opilski, *Materialwissenschaft & Werkstofftechnik* **47**, 5, 1-9 (2016).
- [7] B. Major, R. Major, F. Bruckert, J. M.Lckner, R. Ebner, T. Kusztosz, P. Lacki, *Arch. And Mater.* **53**, 39-48 (2008).
- [8] A. Zieliński, S. Sobieszczyk, B. Świeczko – Żurek, *Inżynieria Materiałowa* **3**, 175, 743-746 (2010).
- [9] E. Krasicka-Cydzik, Anodic layer formation on titanium and its alloy for biomedical applications – Towards Achieving Enhanced Properties fo Diversified Applications, Dr A.K.M. Nurl Am In (Ed.) 2012.
- [10] A. Krzakała, A. Kazek-Kesik, W. Simka, *RSC Adv.*, 3 (2013) 19725-19743.
- [11] T.M. Keaveny, E.F. Morgan, O.C. Yeh, *Bone Mechanics. Standard book of Biomedical Engineering and Design* (2004).
- [12] K. Siamnuai, S. Rooppakhun, *Influence of plate length on the Mechanical performance of dynamic hip screw.* IACSIT Press, Singapore 2012.
- [13] S. Rooppakhun, N.C hantarapanich, B. Chernchujit, B. Mahaisavariya, S. Sucharitpwatskul, K. Sitthiseripratip, *Mechanical Evaluation of Dynamic Hip Screwfor Trochanteric Fracture. International Scholary and Scientific Research & Innovations* **4**, 9 576-579 (2010).
- [14] R. Będziński (red.), *Mechanika techniczna. Biomechanika*, t. XII, Wyd. Instytut Podstawowych Problemów Techniki PAN, Warszawa (2011).
- [15] Z. Horák, M. Hrubina, V. Dzupa, *Bulletin Of Applied Mechanics* **7**, 27 60-65 (2011).
- [16] N.S. Taheri, A.S. Blicblau, M. Singh, *Int. J. Eng Tech.* **1**, 1 141-146 (2012).
- [17] M. Hrubina, Z. Horák, R. Bartoška, L. Navrátil, J. Rosina., *J Appl Biomed.* **11**, 143-151 (2013).
- [18] J. Szewczenko, J. Jaglarz, M. Basiaga, *Opt Appl* **43**, 1 173-180 (2013).
- [19] M. Kiel-Jamrozik, J. Szewczenko, M. Basiaga, *Acta Bioeng Biomech* **17**, 1, 31-37 (2015).
- [20] M. Kiel, J. Szewczenko, J. Marciniak, K. Nowińska: Electrochemical properties of Ti-6Al-4V ELI alloy after anodization, in: E. Piętka, J. Kawa (Ed.): LNCS 7339, Springer-Verlag Berlin Heidelberg (2012).

